J. Fluid Mech. (1982), *vol.* 122, *pp.* 487–504
Printed in Great Britain

Stabilizing effects of finite core on Kármán vortex street

By SHIGEO KIDA

Research Institute for Mathematical Sciences,
Kyoto University, Kyoto 606, Japan

(Received 19 May 1981 and in revised form 9 March 1982)

The stability of a vortex street consisting of two parallel rows of staggered arrangement is investigated by taking account of the effects of the finite core of the vortex. A finite stable region of the transverse-to-longitudinal spacing ratio k is found around 0·281, the value obtained by Kármán. As the core size increases, this stable region moves to larger k. The width of the stable region also changes with the core size S/l^2, where S is the area of the core and l is the longitudinal spacing of the vortex street. It is null at $S/l^2 = 0$, increases at first in proportion to the square of S/l^2, takes a maximum value at $S/l^2 \simeq 0{\cdot}08$, then decreases to zero at $S/l^2 \simeq 0{\cdot}11$. For still larger values of $S/l^2 \gtrsim 0{\cdot}11$, it increases again rather rapidly. The wavenumber of the disturbance having the maximum growth rate is shown to be in complete agreement with that of a growing disturbance recently discovered in a vortex street behind a circular cylinder.

1. Introduction

The regular pattern of a vortex street behind a bluff body at a Reynolds number above a certain critical value has been much investigated both theoretically and experimentally (Wille 1960; Goldstein 1965). Far downstream the vortices arrange themselves in two rows, with opposite signs of circulation. Each vortex is located opposite the midpoint of the interval between the two closest vortices in the opposite row. Taneda (1959) discovered a secondary vortex street re-established after the breakdown of such a (primary) vortex street, which brought about a new interest on this problem.

The linear stability of a system of point vortices in two parallel rows was first considered by Kármán (see Lamb 1932). For two opposite-signed streets of point vortices the symmetric configuration is unconditionally unstable. The asymmetric configuration, on the other hand, is unstable unless the transverse-to-longitudinal spacing ratio $k \equiv h/l$ is equal to $k_c \simeq 0{\cdot}28055$ (where $\sinh \pi k_c = 1$). It was shown later, however, that, even when the spacing ratio takes this value, there will be a weak instability for certain finite disturbances (see Kochin, Kiebel & Roze 1964). Thus as long as the stability analysis is based on point vortices, all double rows of vortices are unstable. This conflicts with the fact that long-lived Kármán vortex streets are observed experimentally.

Domm (1955) investigated the effects of finite cores of vortices on stability by making use of circular vortex tubes, but could not obtain any finite stable region.

Christiansen & Zabusky (1973) studied the time development of a system of vortex tubes of finite core numerically, and found that the finite core has both stabilizing and destabilizing effects. It is a remarkable observation that the finite-area vortex streets have a small stable region around $k = k_c$.

In the present paper we investigate, on the basis of a linear stability theory, the effects of the finite core of the vortex on the stability of a vortex street consisting of two parallel rows of staggered arrangement. We assume that the area S of the vortex core is much smaller than the square of the transverse or longitudinal spacing of the vortex street. The motion of a system of vortex tubes of small core is considered in §2. It is important to note that both the convective velocity of a vortex tube in a given velocity field and the induced velocity of a vortex tube differ from those of a point vortex by the same order, i.e. the order of S^2 (see (2.33) and (2.40)). This law of motion of vortex tubes is used to investigate stability characteristics of a Kármán vortex street of finite core in §3. A finite stable region is found around $k = k_c$. As the core size increases, this stable region moves to the larger part of k. Its width also changes with core size. It is rather small for $S/l^2 \lesssim 0{\cdot}11$, while it increases rapidly with S/l^2 for $S/l^2 \gtrsim 0{\cdot}11$. The wavenumber of the disturbance having the maximum growth rate is shown to be in complete agreement with that of a growing disturbance recently discovered in a vortex street behind a circular cylinder (Okude 1978; Okude & Matsui 1981 private communication). Some remarks about the stability of a Kármán vortex street and the numerical work of Christiansen & Zabusky (1973) are made in §4.

2. Motion of vortex tubes of finite core

We consider the two-dimensional motion of vortex tubes of small finite core in an incompressible and inviscid fluid extending to infinity. It is well known that a point vortex of vanishing core induces a velocity field according to the Biot–Savart law and moves with the velocity at the point vortex induced by the other sources (see Lamb 1932). If the shape of the core of the vortex tube is circular, neither the induced nor convective velocity is affected. The induced velocity due to a vortex tube of circular cross-section is the same as that due to a point vortex located at the centre of the tube and having the same circulation (see (2.38)), and the vortex tube is convected with the velocity at its centre induced by the other sources (see below (2.32)). If the shape of the core deviates from a circle, both the induced and convective velocities are altered. In the following we examine these effects.

Let us consider a vortex tube of finite core in an external shear flow

$$\mathbf{U}(\mathbf{x},t) = [U(\mathbf{x},t), V(\mathbf{x},t)],$$

which is incompressible and irrotational. The cross-sectional area S of the tube is assumed to be small compared with the square of the characteristic length of the external flow. The vorticity ω_0 is distributed uniformly throughout the cross-section and the circulation Γ around the vortex tube is given by $\Gamma = \omega_0 S$. Then, the velocity field $\mathbf{u}(\mathbf{x},t)$ is written as

$$\mathbf{u}(\mathbf{x},t) = \frac{\Gamma}{2\pi S}\iint_S \frac{\hat{\mathbf{z}}\times(\mathbf{x}-\mathbf{x}')}{|\mathbf{x}-\mathbf{x}'|^2}\,d\mathbf{x}' + \mathbf{U}(\mathbf{x},t), \tag{2.1}$$

where $\hat{\mathbf{z}}$ is the unit vector perpendicular to the (x, y)-plane and the integration is carried out over the cross-section of the vortex tube. The position of the tube is defined by the centroid of the vortex region:

$$\mathbf{X} \equiv (X, Y) = \frac{1}{S}\iint_S \mathbf{x}\, d\mathbf{x}. \tag{2.2}$$

The inviscid Navier–Stokes equations for two-dimensional flow are written as

$$\frac{\partial \omega}{\partial t} + \operatorname{div}(\mathbf{u}\,\omega) = 0, \quad \operatorname{div}\mathbf{u} = 0, \tag{2.3}$$

where $\omega(\mathbf{x}, t)$ is the vorticity.

Suppose that there is an isolated region S of vorticity. If we integrate (2.3) multiplied by $\mathbf{x}$ over the domain S, we obtain the convective velocity of this vorticity region:

$$\frac{d\mathbf{X}}{dt} = \frac{1}{S}\iint_S \mathbf{u}(\mathbf{x}, t)\, d\mathbf{x}. \tag{2.4}$$

It follows from (2.1) and (2.4) that

$$\frac{d\mathbf{X}}{dt} = \frac{1}{S}\iint_S \mathbf{U}(\mathbf{x}, t)\, d\mathbf{x}, \tag{2.5}$$

which shows that a vortex region is convected with the velocity induced by the other sources.

Let us express the boundary of the vortex tube by

$$f(\mathbf{x}, t) = 0. \tag{2.6}$$

Since any fluid particle moves with the velocity $\mathbf{u}(\mathbf{x}, t)$, we have the condition

$$\left[\frac{\partial}{\partial t} + (\mathbf{u}.\operatorname{grad})\right] f(\mathbf{x}, t) = 0 \quad \text{on} \quad f(\mathbf{x}, t) = 0. \tag{2.7}$$

We introduce a polar co-ordinate system (r, θ) moving with velocity (2.5):

$$x = X + r\cos\theta, \quad y = Y + r\sin\theta. \tag{2.8}$$

If we denote the r- and θ-components of the velocity in this co-ordinate system by u_r and u_θ, respectively, we have

$$u = \frac{dX}{dt} + u_r\cos\theta - u_\theta\sin\theta, \tag{2.9a}$$

$$v = \frac{dY}{dt} + u_r\sin\theta + u_\theta\cos\theta. \tag{2.9b}$$

Then (2.1) becomes

$$\begin{aligned} u_r(r, \theta; t) = {} & \frac{\Gamma}{2\pi S}\iint_S \frac{r'^2\sin(\theta' - \theta)}{r^2 + r'^2 - 2rr'\cos(\theta' - \theta)}\, dr'\, d\theta' \\ & + \left(U_0 - \frac{dX}{dt}\right)\cos\theta + \left(V_0 - \frac{dY}{dt}\right)\sin\theta \\ & + (A\cos 2\theta + B\sin 2\theta)\, r + (C\cos 3\theta + D\sin 3\theta)\, r^2 + \ldots, \end{aligned} \tag{2.10}$$

$$u_\theta(r,\theta;t)=\frac{\Gamma}{2\pi S}\iint_S\frac{r-r'\cos(\theta'-\theta)}{r^2+r'^2-2rr'\cos(\theta'-\theta)}r'\,dr'\,d\theta'$$
$$-\left(U_0-\frac{dX}{dt}\right)\sin\theta+\left(V_0-\frac{dY}{dt}\right)\cos\theta$$
$$-(A\sin 2\theta-B\cos 2\theta)r-(C\sin 3\theta-D\cos 3\theta)r^2-\ldots. \tag{2.11}$$

We have expanded $\mathbf{U}(\mathbf{x},t)$ around $\mathbf{X}$ as

$$U(\mathbf{x},t)=U_0+(A\cos\theta+B\sin\theta)r+\tfrac{1}{2}(C\cos 2\theta+D\sin 2\theta)r^2+\ldots, \tag{2.12a}$$

$$V(\mathbf{x},t)=V_0+(B\cos\theta-A\sin\theta)r+\tfrac{1}{2}(D\cos 2\theta-C\sin 2\theta)r^2+\ldots, \tag{2.12b}$$

where

$$\left.\begin{aligned}
&U_0=U(\mathbf{X},t),\quad V_0=V(\mathbf{X},t),\\
&A=\frac{\partial}{\partial X}U(\mathbf{X},t)=-\frac{\partial}{\partial Y}V(\mathbf{X},t),\\
&B=\frac{\partial}{\partial Y}U(\mathbf{X},t)=\frac{\partial}{\partial X}V(\mathbf{X},t),\\
&C=\frac{\partial^2}{\partial X^2}U(\mathbf{X},t)=-\frac{\partial^2}{\partial Y^2}U(\mathbf{X},t)=-\frac{\partial^2}{\partial X\partial Y}V(\mathbf{X},t),\\
&D=\frac{\partial^2}{\partial X\partial Y}U(\mathbf{X},t)=\frac{\partial^2}{\partial X^2}V(\mathbf{X},t)=-\frac{\partial^2}{\partial Y^2}V(\mathbf{X},t).
\end{aligned}\right\} \tag{2.13}$$

The dots in (2.10)–(2.12) stand for the higher-order terms with respect to r.

The boundary condition (2.7) converts into

$$\left(\frac{\partial}{\partial t}+u_r\frac{\partial}{\partial r}+\frac{u_\theta}{r}\frac{\partial}{\partial\theta}\right)\tilde{f}(r,\theta;t)=0\quad\text{on}\quad\tilde{f}(r,\theta;t)=0, \tag{2.14}$$

where $\tilde{f}(r,\theta;t)=f(\mathbf{x},t)$.

We now determine the shape and the convective velocity of the vortex tube by a method of perturbation starting from a circular cross-section. The expansion parameter for the perturbation is the smallness of the cross-section compared with the scale of the external flow.

We put

$$\tilde{f}(r,\theta;t)=r-r_b(\theta,t), \tag{2.15}$$

$$r_b(\theta,t)=r_0+r_d(\theta,t). \tag{2.16}$$

Here $r_0\,[=(S/\pi)^{\frac{1}{2}}]$, which is independent of θ and t, represents a circular cross-section of invariant area in the leading order of the perturbation, while $r_d\,(|r_d|\ll r_0)$ represents a deviation from circular form due to the external flow. Then (2.14) is rewritten as

$$\frac{\partial r_d}{\partial t}-u_r(r_b,\theta;t)+\frac{u_\theta(r_b,\theta;t)}{r_0+r_d}\frac{\partial r_d}{\partial\theta}=0. \tag{2.17}$$

We consider the situation where Γ, A, B, C and D are quantities of order one, and r_0, or S, is very small compared with them. Although we do not non-dimensionalize our quantities, we can regard r_0 as an expansion parameter. If we suppose that $r_0\gg|r_d(\theta,t)|$, then the integrals in (2.10) and (2.11) can be calculated successively,

and we find

$$u_r(r_b,\theta;t) = -\frac{\Gamma}{4\pi S}\int_0^{2\pi}\frac{\partial r_d'}{\partial\theta'}\ln[1-\cos(\theta'-\theta)]\,d\theta' + \left(U_0-\frac{dX}{dt}\right)\cos\theta+\left(V_0-\frac{dY}{dt}\right)\sin\theta + (A\cos 2\theta + B\sin 2\theta)\,r_b + (C\cos 3\theta + D\sin 3\theta)\,r_b^2 + O(r_0^3, r_d^2/r_0^3), \quad (2.18)$$

$$u_\theta(r_b,\theta;t) = \frac{\Gamma}{2S}r_0 - \left(U_0-\frac{dX}{dt}\right)\sin\theta+\left(V_0-\frac{dY}{dt}\right)\cos\theta + O(r_0, r_d/r_0^2), \quad (2.19)$$

where $r_d' \equiv r_d(\theta',t)$.

We expand the convective velocity as

$$\frac{d\mathbf{X}}{dt} = \sum_{n=0}^{\infty}\left(\frac{d\mathbf{X}}{dt}\right)^{(n)}, \quad (2.20)$$

where the superscripts denote the order with respect to r_0.

The leading-order term represents the situation where there is no external flow and the shape of the cross-section of the vortex tube is circular. If we neglect r_d, A, B, C and D in (2.17)–(2.19) we get

$$\left(\frac{d\mathbf{X}}{dt}\right)^{(0)} = \mathbf{U}_0. \quad (2.21)$$

Next, we take account of the first-order terms of r_d and the terms containing A and B in (2.18) and (2.19). Then (2.17) gives

$$\frac{\partial r_d}{\partial t}+\frac{\Gamma}{4\pi S}\int_0^{2\pi}\frac{\partial r_d'}{\partial\theta'}\ln[1-\cos(\theta'-\theta)]\,d\theta' + \left(\frac{dX}{dt}\right)^{(1)}\cos\theta+\left(\frac{dY}{dt}\right)^{(1)}\sin\theta-(A\cos 2\theta+B\sin 2\theta)\,r_0+\frac{\Gamma}{2S}\frac{\partial r_d}{\partial\theta}=0. \quad (2.22)$$

We expand $r_d(\theta,t)$ in a Fourier series:

$$r_d(\theta,t) = \sum_{n=2}^{\infty}[a_n(t)\cos n\theta + b_n(t)\sin n\theta]. \quad (2.23)$$

The lack of the $n = 0$ and 1 modes in (2.23) comes from the incompressibility of the fluid and the definition of the centre of the vortex tube (see (2.2) and (2.8)).

Substitution of (2.23) into (2.22) gives

$$\frac{da_n}{dt}+(n-1)\frac{\Gamma}{2S}b_n = A\,r_0\,\delta_{n2}, \quad (2.24a)$$

$$\frac{db_n}{dt}-(n-1)\frac{\Gamma}{2S}a_n = B\,r_0\,\delta_{n2}, \quad (2.24b)$$

$$\left(\frac{d\mathbf{X}}{dt}\right)^{(1)} = 0, \quad (2.25)$$

where δ is the Kronecker δ-symbol.

Equations (2.24a, b) have the following solutions:

$$\left.\begin{aligned} a_2 &= -\frac{2S}{\Gamma} r_0 B + \mathscr{R}\{a_2^{(3)} \exp[it\Gamma/2S]\} + O(r_0^5), \\ b_2 &= \frac{2S}{\Gamma} r_0 A + \mathscr{R}\{b_2^{(3)} \exp[it\Gamma/2S]\} + O(r_0^5), \\ a_n &= \mathscr{R}\{a_n^{(3)} \exp[i(n-1)t\Gamma/2S]\}, \\ b_n &= \mathscr{R}\{b_n^{(3)} \exp[i(n-1)t\Gamma/2S]\} \quad (n = 3, 4, \ldots), \end{aligned}\right\} \tag{2.26}$$

where $a_n^{(3)}$ and $b_n^{(3)}$ $(n = 2, 3, \ldots)$ are constants of integration and are assumed to be $O(r_0^3)$. We have used the condition that S/Γ is much less than the characteristic times of the external flow and the motion of the centroid of the vortex tube. Then we have

$$\begin{aligned} r_{\mathrm{d}} = {} & \frac{2S}{\Gamma} r_0 (A \sin 2\theta - B \cos 2\theta) \\ & + \mathscr{R} \sum_{n=2}^{\infty} (a_n^{(3)} \cos n\theta + b_n^{(3)} \sin n\theta) \exp[i(n-1)t\Gamma/2S] + r_{\mathrm{d}}^{(4)} + \ldots, \end{aligned} \tag{2.27}$$

where $r_{\mathrm{d}}^{(4)}$ is the next-order term, which is $O(r_0^4)$ (see (2.30)).

The equation for $r_{\mathrm{d}}^{(4)}$ is obtained from the next-order terms in (2.17)–(2.19):

$$\begin{aligned} & \frac{\partial r_{\mathrm{d}}^{(4)}}{\partial t} + \frac{\Gamma}{4\pi S} \int_0^{2\pi} \frac{\partial r_{\mathrm{d}}^{(4)\prime}}{\partial \theta'} \ln[1 - \cos(\theta' - \theta)]\, d\theta' \\ & + \left(\frac{dX}{dt}\right)^{(2)} \cos\theta + \left(\frac{dY}{dt}\right)^{(2)} \sin\theta - (C \cos 3\theta + D \sin 3\theta) r_0^2 + \frac{\Gamma}{2S} \frac{\partial r_{\mathrm{d}}^{(4)}}{\partial \theta} = 0. \end{aligned} \tag{2.28}$$

In just the same way as for (2.22) we find

$$\left(\frac{d\mathbf{X}}{dt}\right)^{(2)} = 0, \tag{2.29}$$

$$r_{\mathrm{d}}^{(4)}(\theta, t) = -\frac{S}{\Gamma} r_0^2 (C \sin 3\theta - D \cos 3\theta). \tag{2.30}$$

The free-oscillation terms have been included in the summation of (2.27).

It follows from (2.16), (2.27) and (2.30) that the shape of the vortex tube is written as

$$\begin{aligned} r_{\mathrm{b}}(\theta, t) = {} & r_0 + \frac{2Sr_0}{\Gamma} (A \sin 2\theta - B \cos 2\theta) \\ & + \mathscr{R} \sum_{n=2}^{\infty} (a_n^{(3)} \cos n\theta + b_n^{(3)} \sin n\theta) \exp[i(n-1)t\Gamma/2S] \\ & + \frac{Sr_0^2}{\Gamma} (C \sin 3\theta - D \cos 3\theta) + O(r_0^5). \end{aligned} \tag{2.31}$$

Thus the shape of the vortex tube oscillates rapidly around that determined by the instantaneous external velocity field.

Incidentally, the steady form of an elliptic vortex of uniform vorticity and its orientation in a steady uniform shear flow are already known (Moore & Saffman 1971; Kida 1981). We can check that if the external flow is steady the second term in (2.31) agrees with the steady elliptic vortex in the limit of small deviations from a circular form.

Now that the shape of the vortex tube has been obtained, we can calculate the convective and induced velocities of a vortex tube. First, we calculate the convective velocity (2.5) of a vortex tube. Equations (2.25) and (2.29) imply that the convective velocity of a vortex tube is not affected to $O(r_0^2)$ by the external flow. In fact, as will be shown in the following, the correction of the convective velocity due to the external flow appears in $O(r_0^4)$. We rewrite (2.5) as

$$\frac{d\mathbf{X}}{dt} = \frac{1}{S}\int_0^{2\pi} d\theta \int_0^{r_a} dr\, r\mathbf{U}(r,\theta;t) + \frac{1}{S}\int_0^{2\pi} d\theta \int_{r_a}^{r_b} dr\, r\mathbf{U}(r,\theta;t), \tag{2.32}$$

where

$$\mathbf{U}(r,\theta;t) \equiv \mathbf{U}(\mathbf{x},t).$$

The first integral in (2.32) represents the average of an incompressible and irrotational flow over a circular domain and is equal to the velocity at the centre of the circular domain owing to the mean-value property of a harmonic function (see e.g. Ahlfors 1966). The second integral can be calculated by making use of the Taylor expansion (2.12) of the velocity field and the shape of the vortex tube (2.31). After some manipulation we obtain

$$\frac{dX}{dt} = U(\mathbf{X},t) + \frac{S^2}{\pi\Gamma}\left(\frac{\partial U}{\partial X}\frac{\partial^2 U}{\partial X\,\partial Y} - \frac{\partial U}{\partial Y}\frac{\partial^2 U}{\partial X^2}\right), \tag{2.33a}$$

$$\frac{dY}{dt} = V(\mathbf{X},t) - \frac{S^2}{\pi\Gamma}\left(\frac{\partial U}{\partial X}\frac{\partial^2 U}{\partial X^2} + \frac{\partial U}{\partial Y}\frac{\partial^2 U}{\partial X\,\partial Y}\right), \tag{2.33b}$$

where the neglected terms are $O(r_0^5)$.†

Next, we calculate the induced velocity due to a vortex tube of finite cross-section S, which is given by the first term of (2.1):

$$\mathbf{u}(\mathbf{x},t) = \frac{\Gamma}{2\pi S}\iint_S \frac{\hat{\mathbf{z}}\times(\mathbf{x}-\mathbf{x}')}{|\mathbf{x}-\mathbf{x}'|^2}\,d\mathbf{x}'. \tag{2.34}$$

Let us divide the domain of integration into two parts: a circular domain S_0 of radius $\tilde{r}_0$ and the remainder $S-S_0$:

$$\mathbf{u}(\mathbf{x},t) = \mathbf{u}_0(\mathbf{x},t) + \mathbf{u}_1(\mathbf{x},t), \tag{2.35}$$

$$\mathbf{u}_0(\mathbf{x},t) = \frac{\Gamma}{2\pi S}\iint_{S_0} \frac{\hat{\mathbf{z}}\times(\mathbf{x}-\mathbf{x}')}{|\mathbf{x}-\mathbf{x}'|^2}\,d\mathbf{x}', \tag{2.36}$$

$$\mathbf{u}_1(\mathbf{x},t) = \frac{\Gamma}{2\pi S}\iint_{S-S_0} \frac{\hat{\mathbf{z}}\times(\mathbf{x}-\mathbf{x}')}{|\mathbf{x}-\mathbf{x}'|^2}\,d\mathbf{x}'. \tag{2.37}$$

We have used the abbreviation

$$\iint_{S-S_0} d\mathbf{x}' \equiv \iint_S d\mathbf{x}' - \iint_{S_0} d\mathbf{x}'.$$

† Strictly speaking, there are rapidly oscillating terms $O(r_0^4)$ whose frequency is $\Gamma/2S$. If we take an average of (2.33) over a time interval that is much longer than the period of this oscillation but much shorter than the characteristic time of the external flow, then these terms become $O(r_0^5)$. Equations (2.33), (2.40), (3.2) and (3.3) should be regarded as such coarse-grained equations with respect to time.

If the centre of the vortex tube is at the origin, then the integral (2.36) is calculated to be

$$\mathbf{u}_0(\mathbf{x},t) = \frac{\Gamma}{2\pi}\frac{\hat{\mathbf{z}}\times\mathbf{x}}{|\mathbf{x}|^2}, \tag{2.38}$$

which shows that a vortex tube of circular cross-section can be replaced by a point vortex having the same circulation.

If we expand $1/|\mathbf{x}-\mathbf{x}'|^2$ in a power series of $\mathbf{x}'$, then the integral (2.37) can be written as

$$\begin{aligned}\mathbf{u}_1(\mathbf{x},t) = {}& \frac{\Gamma}{2\pi S}\iint_{S-S_0}\frac{\hat{\mathbf{z}}\times\mathbf{x}}{|\mathbf{x}|^2}d\mathbf{x}' \\ & + \frac{\Gamma}{2\pi S}\hat{\mathbf{z}}\times\iint_{S-S_0}\left(\frac{2\mathbf{x}(\mathbf{x}.\mathbf{x}')}{|\mathbf{x}|^4}-\frac{\mathbf{x}'}{|\mathbf{x}|^2}\right)d\mathbf{x}' \\ & + \frac{\Gamma}{2\pi S}\hat{\mathbf{z}}\times\iint_{S-S_0}\left(\frac{4\mathbf{x}(\mathbf{x}.\mathbf{x}')^2}{|\mathbf{x}|^6}-\frac{\mathbf{x}|\mathbf{x}'|^2}{|\mathbf{x}|^4}-\frac{2\mathbf{x}'(\mathbf{x}.\mathbf{x}')}{|\mathbf{x}|^4}\right)d\mathbf{x}'. \end{aligned} \tag{2.39}$$

The first and second integrals of (2.39) vanish because the areas of S and S_0 are equal and the centre of the vortex tube lies at the origin. The third integral can be calculated explicitly when the shape of the vortex tube is given by (2.31). After some calculation we find

$$u(\mathbf{x},t) = -\frac{\Gamma}{2\pi}\frac{y}{|\mathbf{x}|^2}+\frac{S^2}{\pi^2|\mathbf{x}|^6}\left[\left(\frac{\partial U}{\partial x}\right)_0(x^2-3y^2)x+\left(\frac{\partial U}{\partial y}\right)_0(3x^2-y^2)y\right], \tag{2.40a}$$

$$v(\mathbf{x},t) = \frac{\Gamma}{2\pi}\frac{x}{|\mathbf{x}|^2}+\frac{S^2}{\pi^2|\mathbf{x}|^6}\left[\left(\frac{\partial U}{\partial x}\right)_0(3x^2-y^2)y-\left(\frac{\partial U}{\partial y}\right)_0(x^2-3y^2)x\right], \tag{2.40b}$$

where $(\partial U/\partial x)_0$ and $(\partial U/\partial y)_0$ are the derivatives of the x-component of velocity at the centre of the vortex tube induced by the other sources. The neglected terms in (2.40) are $O(r_0^5)$ (see the footnote to (2.33)). Note that (2.40) contains only the first derivatives of the external velocity with respect to the space co-ordinates and agrees with the velocity field induced by a slightly elliptical vortex (Moore & Saffman 1971).

3. Stability of a Kármán vortex street

An analysis based on point vortices of vanishing core revealed that an asymmetric configuration as shown in figure 1 is stable only when the transverse-to-longitudinal spacing ratio $k \equiv h/l$ takes a special value k_c (Lamb 1932). We are interested in the problem of whether there appears a finite stable region around $k = k_c$ if effects of finite core of vortex tubes are taken into account.

We consider an asymmetric configuration of double rows of vortex tubes of finite core. The distance between the two rows is h and that between consecutive vortices in the same row is l. The areas S of the cores are assumed to be common and much less than l^2. A physical requirement that the neighbouring vortex tubes must not overlap is

$$P \equiv \frac{S}{l^2} \leqslant \tfrac{1}{4}\pi \min(1, \tfrac{1}{4}+k^2), \tag{3.1}$$

if the cores of the tubes are approximated by circles. The vorticity is assumed to be uniformly distributed throughout the core. All the vortex tubes in the upper row have

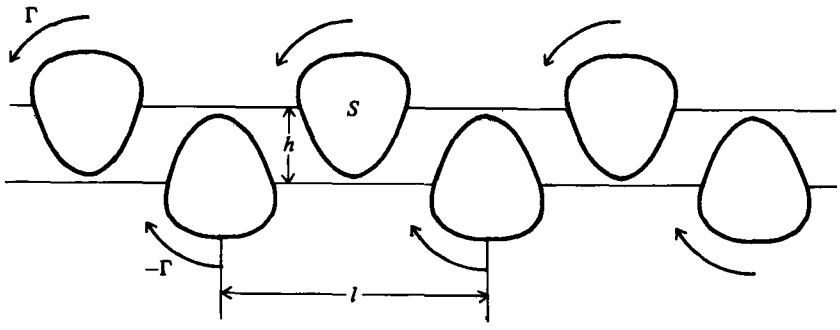

FIGURE 1. A Kármán vortex street of finite core;
$h/l = k_0 \simeq 0{\cdot}28055$, $(S/l^2)^{\frac{1}{2}} = 0{\cdot}02$.

the same circulation Γ and those in the lower row the opposite circulation $-\Gamma$. Let the perturbations of the centres of vortex tubes in the upper row be (x_m, y_m) and those in the lower (x'_n, y'_n); then the co-ordinates of the centres of the vortex tubes in the upper row are $(ml+Vt+x_m, \frac{1}{2}h+y_m)$ and those in the lower $[(n+\frac{1}{2})l+Vt+x'_n, -\frac{1}{2}h+y'_n]$, where m and n are integers and V denotes the velocity of advance of the Kármán vortex street.

The equation of motion of the centre of the vortex tube corresponding to $m = 0$ can be derived by making use of (2.33) and (2.40):

$$\begin{aligned}\frac{dx_0}{dt}+V = &-\frac{\Gamma}{2\pi}\sum_{m(\neq 0)}\frac{\bar{y}_{m0}}{r_{m0}^2}+\frac{\Gamma}{2\pi}\sum_n\frac{\bar{y}'_{n0}}{r'^2_{n0}}\\ &+\frac{S^2}{\pi^2}\sum_{m(\neq 0)}\left[\frac{\partial u_m}{\partial x_m}(\bar{x}^2_{m0}-3\bar{y}^2_{m0})\,\bar{x}_{m0}+\frac{\partial u_m}{\partial y_m}(3\bar{x}^2_{m0}-\bar{y}^2_{m0})\,\bar{y}_{m0}\right]\Big/ r^3_{m0}\\ &+\frac{S^2}{\pi^2}\sum_n\left[\frac{\partial u'_n}{\partial x_n}(\bar{x}'^2_{n0}-3\bar{y}'^2_{n0})\,\bar{x}'_{n0}+\frac{\partial u'_n}{\partial y_n}(3\bar{x}'^2_{n0}-\bar{y}'^2_{n0})\,\bar{y}'_{n0}\right]\Big/ r'^3_{n0}\\ &+\frac{S^2}{\pi\Gamma}\left(\frac{\partial u_0}{\partial x_0}\frac{\partial^2 u_0}{\partial x_0\partial y_0}-\frac{\partial u_0}{\partial y_0}\frac{\partial^2 u_0}{\partial x_0^2}\right),\end{aligned} \tag{3.2}$$

$$\begin{aligned}\frac{dy_0}{dt} = &\frac{\Gamma}{2\pi}\sum_{m(\neq 0)}\frac{\bar{x}_{m0}}{r_{m0}^2}-\frac{\Gamma}{2\pi}\sum_n\frac{\bar{x}'_{n0}}{r'^2_{n0}}\\ &+\frac{S^2}{\pi^2}\sum_{m(\neq 0)}\left[\frac{\partial u_m}{\partial x_m}(3\bar{x}^2_{m0}-\bar{y}^2_{n0})\,\bar{y}_{m0}-\frac{\partial u_m}{\partial y_m}(\bar{x}^2_{m0}-3\bar{y}^2_{m0})\,\bar{x}_{m0}\right]\Big/ r^3_{m0}\\ &+\frac{S^2}{\pi^2}\sum_n\left[\frac{\partial u'_n}{\partial x_n}(3\bar{x}'^2_{n0}-\bar{y}'^2_{n0})\,\bar{y}'_{n0}-\frac{\partial u'_n}{\partial y_n}(\bar{x}'^2_{n0}-3\bar{y}'^2_{n0})\,\bar{x}'_{n0}\right]\Big/ r'^3_{n0}\\ &-\frac{S^2}{\pi\Gamma}\left(\frac{\partial u_0}{\partial x_0}\frac{\partial^2 u_0}{\partial x_0^2}+\frac{\partial u_0}{\partial y_0}\frac{\partial^2 u_0}{\partial x_0\partial y_0}\right),\end{aligned} \tag{3.3}$$

where

$$u_{m'} = -\frac{\Gamma}{2\pi}\sum_{m(\neq m')}\frac{\bar{y}_{mm'}}{r^2_{mm'}}+\frac{\Gamma}{2\pi}\sum_n\frac{\bar{y}'_{nm'}}{r'^2_{nm'}}, \tag{3.4}$$

$$\left.\begin{aligned}&\bar{x}_{mm'} = x_{m'}-x_m+(m'-m)l, \quad \bar{y}_{mm'} = y_{m'}-y_m,\\ &\bar{x}'_{nm} = x_m-x'_n+(m-n-\tfrac{1}{2})l, \quad \bar{y}'_{nm} = y_m-y'_n+h,\\ &r_{mm'} = (\bar{x}^2_{mm'}+\bar{y}^2_{mm'})^{\frac{1}{2}}, \quad r'_{nm} = (\bar{x}'^2_{nm}+\bar{y}'^2_{nm})^{\frac{1}{2}}.\end{aligned}\right\} \tag{3.5}$$

The velocity (3.4) is the first-order approximation of the x-component of the velocity at the centre of the m'th vortex tube in the upper row induced by all the other vortex tubes. The velocity $u'_{n'}$ of the n'th vortex tube in the lower row is obtained from (3.4) by the following transformation:

$$m \rightleftarrows n, \quad m' \to n', \quad \Gamma \to -\Gamma, \quad h \to -h, \quad x \rightleftarrows x', \quad y \rightleftarrows y'.$$

The velocity of advance V is obtained from (3.2) by setting the perturbation equal to zero:

$$V = \frac{\Gamma}{2l}\tanh \pi k \left[1 - \frac{2\pi^2 S^2}{l^4}\operatorname{sech}^2 \pi k \,(\operatorname{sech}^2 \pi k - \tfrac{1}{3})\right]. \tag{3.6}$$

The second term represents a correction due to the finite core of the vortex tubes.

Let the perturbation (x_m, y_m) and (x'_n, y'_n) be so small in magnitude compared with l that the linearization of the system (3.2) and (3.3) is permissible; and let us consider a perturbation of the type

$$\begin{bmatrix} x_m \\ y_m \end{bmatrix} = \begin{bmatrix} \alpha \\ \beta \end{bmatrix} \exp\left[i(m\phi - \lambda t)\right], \tag{3.7a}$$

$$\begin{bmatrix} x'_n \\ y'_n \end{bmatrix} = \begin{bmatrix} \alpha' \\ \beta' \end{bmatrix} \exp\left\{i[(n+\tfrac{1}{2})\,\phi - \lambda t]\right\}, \tag{3.7b}$$

where α, β, α', β', ϕ and λ are constants. ϕ represents the wavenumber of the perturbation, and may be assumed to lie between 0 and 2π. The imaginary part of λ represents the growth rate of the perturbation; the vortex street is stable or unstable according to whether it is zero or non-zero.

Introducing these forms into the linearized equations of (3.2) and (3.3), we obtain

$$\begin{bmatrix} i(A_1+\Lambda) & -(B_0+B_1) & -i(C_0+C_1) & -(D_0+D_1) \\ -(B_0+B_2) & i(A_2+\Lambda) & -(D_0+D_2) & i(C_0+C_2) \\ -i(C_0+C_1) & D_0+D_1 & i(A_1+\Lambda) & B_0+B_1 \\ D_0+D_2 & i(C_0+C_2) & B_0+B_2 & i(A_2+\Lambda) \end{bmatrix} \begin{bmatrix} \alpha \\ \beta \\ \alpha' \\ \beta' \end{bmatrix} = 0, \tag{3.8}$$

where

$$\Lambda = \frac{2\pi l^2}{\Gamma}\lambda, \tag{3.9}$$

$$A_1 = \frac{P^2}{2\pi^2}(-2EG + 3IJ - CI/k), \quad A_2 = \frac{P^2}{2\pi^2}(-2EG + IJ), \tag{3.10), (3.11}$$

$$B_1 = -\frac{P^2}{2\pi^2}(E^2 + G^2 + I^2 + 2J^2 - FH - CJ/k), \tag{3.12}$$

$$B_2 = \frac{P^2}{2\pi^2}(E^2 + G^2 + I^2 + FH), \tag{3.13}$$

$$C_1 = \frac{P^2}{2\pi^2}(EJ - FK - CE/k), \quad C_2 = \frac{P^2}{2\pi^2}(EJ - FK), \tag{3.14), (3.15}$$

$$D_1 = \frac{P^2}{2\pi^2}(2EI - FL + 3GJ - CG/k), \quad D_2 = -\frac{P^2}{2\pi^2}(2EI + FL + GJ), \tag{3.16), (3.17}$$

$$B_0 = \sum_{m(\neq 0)} \frac{1}{m^2}(1-e^{im\phi}) - \sum_n \frac{(n+\frac{1}{2})^2-k^2}{[(n+\frac{1}{2})^2+k^2]^2} = \tfrac{1}{2}\phi(2\pi-\phi) - \pi^2 \operatorname{sech}^2 \pi k, \tag{3.18}$$

$$C_0 = -i\sum_n \frac{2(n+\frac{1}{2})k}{[(n+\frac{1}{2})^2+k^2]^2} \exp[i(n+\tfrac{1}{2})\phi] = \pi\left(\pi \frac{\sinh \phi k}{\cosh^2 \pi k} + \phi \frac{\sinh(\pi-\phi)k}{\cosh \pi k}\right), \tag{3.19}$$

$$D_0 = \sum_n \frac{(n+\frac{1}{2})^2-k^2}{[(n+\frac{1}{2})^2+k^2]^2} \exp[i(n+\tfrac{1}{2})\phi] = \pi\left(\pi \frac{\cosh \phi k}{\cosh^2 \pi k} - \phi \frac{\cosh(\pi-\phi)k}{\cosh \pi k}\right), \tag{3.20}$$

$$E = \sum_n \frac{2k[3(n+\frac{1}{2})^2-k^2]}{[(n+\frac{1}{2})^2+k^2]^3} = 2\pi^3 \tanh \pi k \operatorname{sech}^2 \pi k, \tag{3.21}$$

$$F = -\sum_{m(\neq 0)} \frac{1}{m^2} + \sum_n \frac{(n+\frac{1}{2})^2-k^2}{[(n+\frac{1}{2})^2+k^2]^2} = \pi^2(\operatorname{sech}^2 \pi k - \tfrac{1}{3}), \tag{3.22}$$

$$G = -i\sum_{m(\neq 0)} \frac{2}{m^3} e^{im\phi} = \tfrac{1}{3}[\pi^3 - \pi^2\phi + (\phi-\pi)^3], \tag{3.23}$$

$$\begin{aligned} H &= -\sum_{m(\neq 0)} \frac{12}{m^4}(1-e^{im\phi}) + \sum_n \frac{12[(n+\frac{1}{2})^4 - 6(n+\frac{1}{2})^2k^2 + k^4]}{[(n+\frac{1}{2})^2+k^2]^4} \\ &= -\tfrac{1}{2}\phi^2(2\pi-\phi)^2 + 4\pi^4(1-3\tanh^2 \pi k)\operatorname{sech}^2 \pi k, \end{aligned} \tag{3.24}$$

$$\begin{aligned} I &= \sum_n \frac{2k[3(n+\frac{1}{2})^2-k^2]}{[(n+\frac{1}{2})^2+k^2]^3} \exp[i(n+\tfrac{1}{2})\phi] \\ &= \pi\left[-\phi^2 \frac{\sinh(\pi-\phi)k}{\cosh \pi k} - 2\pi\phi \frac{\sinh \phi k}{\cosh^2 \pi k} + 2\pi^2 \frac{\cosh \phi k \sinh \pi k}{\cosh^3 \pi k}\right], \end{aligned} \tag{3.25}$$

$$\begin{aligned} J &= -i\sum_n \frac{2(n+\frac{1}{2})[(n+\frac{1}{2})^2-3k^2]}{[(n+\frac{1}{2})^2+k^2]^3} \exp[i(n+\tfrac{1}{2})\phi] \\ &= \pi\left[-\phi^2 \frac{\cosh(\pi-\phi)k}{\cosh \pi k} + 2\pi\phi \frac{\cosh \phi k}{\cosh^2 \pi k} - 2\pi^2 \frac{\sinh \phi k \sinh \pi k}{\cosh^3 \pi k}\right], \end{aligned} \tag{3.26}$$

$$\begin{aligned} K &= -i\sum_n \frac{48(n+\frac{1}{2})k[(n+\frac{1}{2})^2-k^2]}{[(n+\frac{1}{2})^2+k^2]^4} \exp[i(n+\tfrac{1}{2})\phi] \\ &= 2\pi\left[\phi^3 \frac{\sinh(\pi-\phi)k}{\cosh \pi k} + 3\pi\phi^2 \frac{\sinh \phi k}{\cosh^2 \pi k}\right. \\ &\quad \left. - 6\pi^2\phi \frac{\cosh \phi k \sinh \pi k}{\cosh^3 \pi k} - 2\pi^3 \frac{\sinh \phi k}{\cosh^2 \pi k}(1-3\tanh^2 \pi k)\right], \end{aligned} \tag{3.27}$$

$$\begin{aligned} L &= \sum_n \frac{12[(n+\frac{1}{2})^4 - 6(n+\frac{1}{2})^2k^2 + k^4]}{[(n+\frac{1}{2})^2+k^2]^4} \exp[i(n+\tfrac{1}{2})\phi] \\ &= 2\pi\left[\phi^3 \frac{\cosh(\pi-\phi)k}{\cosh \pi k} - 3\pi\phi^2 \frac{\cosh \phi k}{\cosh^2 \pi k}\right. \\ &\quad \left. + 6\pi^2\phi \frac{\sinh \phi k \sinh \pi k}{\cosh^3 \pi k} + 2\pi^3 \frac{\cosh \phi k}{\cosh^2 \pi k}(1-3\tanh^2 \pi k)\right], \end{aligned} \tag{3.28}$$

Equations for α' and β' have been derived from those for α and β by reversing the signs of Γ and k and interchanging primed and unprimed letters.

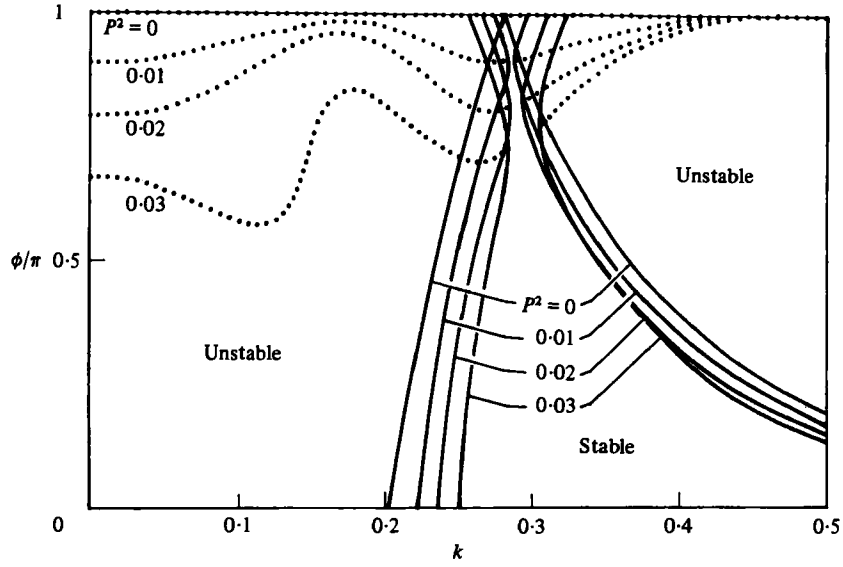

FIGURE 2. Stability diagram for a Kármán vortex street of finite core. The solid curves indicate the stability boundaries and the dotted lines the wavenumbers of disturbances having the maximum growth rate for given k and P.

In order that (3.8) have non-trivial solutions, the determinant of the matrix of the coefficients must be zero:

$$(\Lambda \pm C_0)^2 - [A_1 + A_2 \pm (C_1 + C_2)](\Lambda \pm C_0) + [B_0 + B_1 \pm (D_0 + D_1)][B_0 + B_2 \mp (D_0 + D_2)] = 0. \quad (3.29)$$

This is a quadratic equation for Λ having real coefficients. The stability condition is that Λ be real, i.e. that the discriminant of (3.29) be non-negative:

$$[A_1 + A_2 \pm (C_1 + C_2)]^2 - 4[B_0 + B_1 \pm (D_0 + D_1)][B_0 + B_2 \mp (D_0 + D_2)] \geqslant 0$$

or

$$4[(D_0 + D_1)(D_0 + D_2) - (B_0 + B_1)(B_0 + B_2)] + (C_1 + C_2)^2 + (A_1 + A_2)^2 \geqslant 2|(C_1 + C_2)(A_1 + A_2) + 2(B_0 + B_1)(D_0 + D_2) - 2(B_0 + B_2)(D_0 + D_1)|. \quad (3.30)$$

The stability characteristics of a Kármán vortex street are shown for various values of P and for $0 \leqslant \phi \leqslant \pi$ in figure 2. The solid curves indicate the stability boundaries given by (3.30). Note that the stability characteristics are symmetric in ϕ about $\phi = \pi$, since the functions B_1, B_2, C_1, C_2, B_0, C_0, E, F, H, J, K are symmetric and A_1, A_2, D_1, D_2, D_0, G, I, L are antisymmetric. In order that a vortex street of spacing ratio k may be stable against any small disturbance, it must be stable for all ϕ at fixed k. For $P = 0$ (the point-vortex approximation) only a single value $k = k_c$ is stable. For finite P, on the other hand, there appears a finite stable region around $k = k_c$. It is seen that the finite core of vortex tubes has a stabilizing effect on disturbances of larger values of ϕ but a destabilizing effect on those of smaller values of ϕ.

When $k \to \infty$, the stability boundary for $P = 0$ approaches the curve

$$\phi = 4\pi \exp(-\pi k). \quad (3.31)$$

This implies that a single row of a vortex street ($k = \infty$) is unstable for all ϕ.

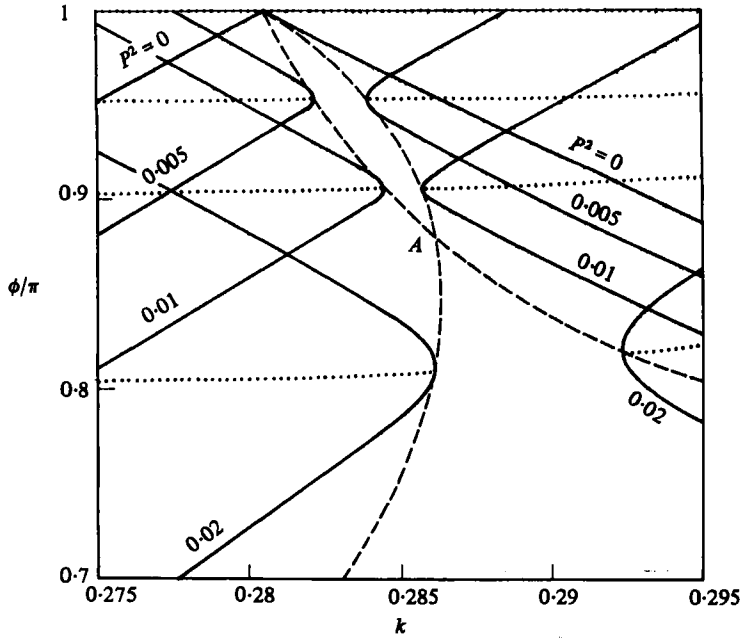

FIGURE 3. Stability diagram near $k = k_c$ and $\phi = \pi$. The solid curves indicate the stability boundaries and the dotted lines the wavenumbers of disturbances having the maximum growth rate for given k and P. The dashed curves are the loci of the extremal points of the stability boundaries. The point $A = (0{\cdot}28619, 0{\cdot}8801)$.

The dotted lines in figure 2 indicate the wavenumbers of disturbances having the maximum growth rates for fixed k and P. When $P = 0$ these wavenumbers are equal to π for all k, i.e. the disturbances whose wavelengths are double the longitudinal spacing of a vortex street grow most rapidly. For finite P, however, these wavenumbers deviate from π, and the disturbances of wavelengths other than double the longitudinal spacing determine the stability condition of a vortex street.

A strange wavenumber of a growing disturbance, $2\pi \times 250/420 \simeq 1{\cdot}19\pi$, was discovered by Okude (1978) in a Kármán vortex street behind a circular cylinder. The origin of this mode may be explained by the present theory as follows. It was shown recently by Okude & Matsui (1981 private communication) that the velocity distribution across this vortex street is well approximated by Rankine vortices. Their data at a distance of 20 diameters downstream of the cylinder are consistent with the choice of the parameters $P^2 \simeq 0{\cdot}02$ and $k \simeq 0{\cdot}28$. The wavenumbers of disturbances having the maximum growth rate are then given by

$$\phi \simeq (1 \pm 0{\cdot}19)\pi \tag{3.32}$$

(see figure 3 or (3.35)). The upper sign of (3.32) coincides with the experimental value $1{\cdot}19\pi$. It is not known, however, why the disturbance of the wavenumber corresponding to the lower sign has not been detected in their experiment.

A close-up near $k = k_c$ and $\phi = \pi$ is shown in figure 3. The stability boundary for a finite P has extremal values of k at two points. If we denote these two points by $[k_\pm(P), \phi_\pm(P)]$, where $k_-(P) \leqslant k_+(P)$, then the stable region of a vortex street is expressed as

$$k_-(P) \leqslant k \leqslant k_+(P). \tag{3.33}$$

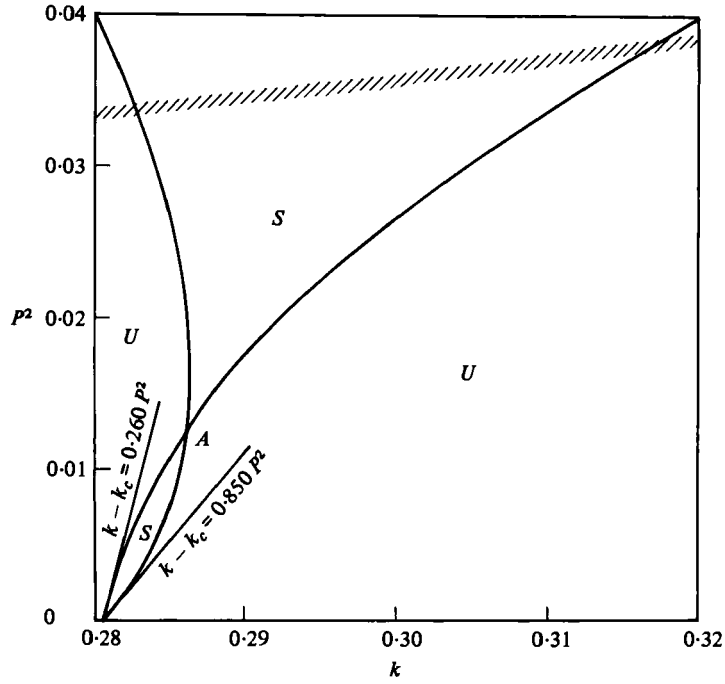

FIGURE 4. Stability diagram in the area–spacing-ratio (P^2, k)-plane. S, stable region; U, unstable region. The point $A = (0{\cdot}28619, 0{\cdot}0127)$. This diagram may be reliable at least below the hatched band.

The functions $\phi_\pm(P)$ represent the wavenumbers of the most-unstable disturbances that determine the stability condition of a vortex street. The dashed curves in figure 3 are the loci of $[k_\pm(P), \phi_\pm(P)]$. They meet at $k \simeq 0{\cdot}28619$ and $\phi/\pi \simeq 0{\cdot}8801$ when $P^2 \simeq 0{\cdot}0127$.

In the vicinity of $k = k_c$ and $\phi = \pi$, the stable condition (3.30) is written as

$$[\sqrt{\tfrac{1}{2}}\pi(k-k_c) - \tfrac{1}{8}\pi^2P^2]^2 - \left[(\sqrt{\tfrac{1}{2}} - \tfrac{1}{2}\pi k_c)\left|\frac{\phi}{\pi} - 1\right| - \tfrac{1}{4}\pi^2P^2\right]^2 - \left(1 - \frac{3\sqrt{2}}{8\pi k_c}\right)^2 (\tfrac{1}{8}\pi^2P^2)^2 \leqslant 0, \tag{3.34}$$

i.e. the boundary is approximated by a hyperbola. Then we have

$$\phi_\pm(P) = \pi\left(1 \pm \frac{\pi^2P^2}{2(\sqrt{2} - \pi k_c)}\right) \simeq \pi[1 \pm 9{\cdot}26P^2], \tag{3.35}$$

$$k_+(P) - k_c = \tfrac{1}{24}\pi\left(7\sqrt{2} - \frac{3}{\pi k_c}\right)P^2 \simeq 0{\cdot}850P^2, \tag{3.36a}$$

$$k_-(P) - k_c = \tfrac{1}{24}\pi\left(\frac{3}{\pi k_c} - \sqrt{2}\right)P^2 \simeq 0{\cdot}260P^2. \tag{3.36b}$$

The functions $k_\pm(P)$ increase with P, and therefore the stable region moves to the larger part of k as P increases.

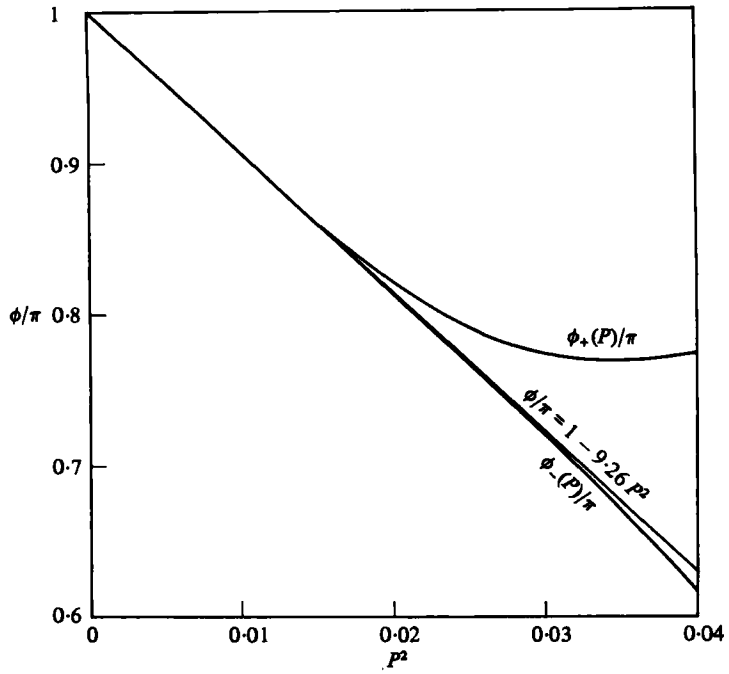

FIGURE 5. The wavenumbers of the most-unstable disturbances $\phi_\pm(P)$.

Incidentally, by putting $\phi = \pi$ in (3.34), we get the stable condition for special disturbances of wavenumber π as follows:

$$\tfrac{1}{8}\sqrt{2}\,\pi\left\{1-\left[4+\frac{16}{9}\left(1-\frac{3\sqrt{2}}{8\pi k_c}\right)^2\right]^{\frac{1}{2}}\right\}P^2 \leqslant k-k_c \leqslant \tfrac{1}{8}\sqrt{2}\,\pi\left\{1+\left[4+\frac{16}{9}\left(1-\frac{3\sqrt{2}}{8\pi k_c}\right)^2\right]^{\frac{1}{2}}\right\}P^2$$

or
$$-0{\cdot}5938P^2 \lesssim k-k_c \lesssim 1{\cdot}705P^2. \tag{3.37}$$

The functions $k_\pm(P)$ are plotted in figure 4, where S and U denote respectively the stable and unstable regions of a vortex street. The two straight lines are the asymptotes (3.36) for very small P. This diagram may be reliable at least below the hatched band, the centreline of which corresponds to the configuration in which

$$\frac{\text{the effective diameter of the vortex tube}}{\text{the distance between the centres of nearest vortex tubes}} = \frac{2r_0}{(\frac{1}{4}+k^2)^{\frac{1}{2}}l} = 2^{-\frac{1}{2}},$$

or
$$P = \tfrac{1}{4}\sqrt{\tfrac{1}{2}}\,\pi(\tfrac{1}{4}+k^2) \quad (\equiv P_m, \text{say}) \tag{3.38}$$

(cf. the discussion concerning figure 6).

As the area of the core increases, the stable region moves to the larger part of k as a whole. The width of the stable region, $k_+(P)-k_-(P)$, is zero at $P = 0$. This width increases at first in proportion to the square of P like (3.36), takes a maximum value at $P^2 \simeq 0{\cdot}006$, then decreases, and vanishes at $P^2 \simeq 0{\cdot}0127$ and $k \simeq 0{\cdot}28619$, but beyond this point it increases again rather rapidly.

The wavenumbers $\phi_\pm(P)$ of the most-unstable disturbances that determine the stability condition are depicted in figure 5. When $P = 0$, both of them are equal to π,

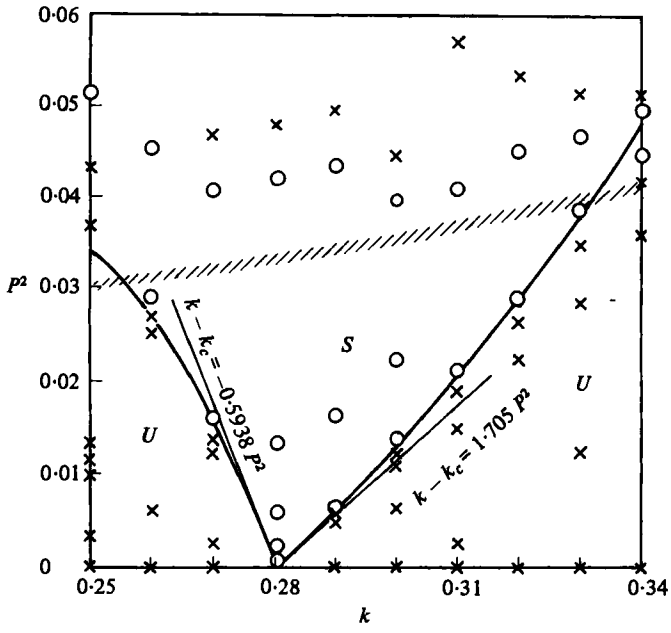

FIGURE 6. Stability diagram for the disturbances of wavenumber π. The solid curves are the stable/unstable boundaries. S, stable region; U, unstable region. The symbols ○ and × indicate stable and unstable states according to Saffman & Schatzman (1982). The present results (the solid curves) agree well with their results, at least below the hatched band.

i.e. the most-unstable modes are the disturbances whose wavelengths are double the longitudinal spacing of a vortex street. For finite P, however, these wavenumbers deviate from π. They change almost linearly with P^2 according to (3.35) for $P^2 \leqslant 0{\cdot}016$.

Recently Saffman & Schatzman (1982) attacked the same problem by solving numerically the linear evolution equations of disturbances of a special wavenumber π for various values of P and k. In their theory P does not need to be small. The results of their stability calculations are plotted in figure 6, which is reproduced using the data in table 1 of their paper. The circles and crosses indicate the stable and unstable states, respectively. We can see a triangular stable region that is limited by two boundaries for a given k. The upper boundary lies somewhere around $0{\cdot}04 \lesssim P^2 \lesssim 0{\cdot}06$, while the lower one increases with $|k-k_c|$. They seem to meet at $k \simeq 0{\cdot}24$ and $0{\cdot}35$.

Unfortunately, however, as stated before, the disturbances of wavenumber π are not the most-unstable modes for finite P, and their results never give the stability condition of a Kármán vortex street of finite core.

The thick solid lines in figure 6 are the stability boundaries of this particular mode from the present theory, which is obtained by putting $\phi = \pi$ in (3.30). They represent the lower boundary well, at least up to the hatched band, the centreline of which is given by (3.38). For very small P, the lower boundary is expressed by (3.37), which is identical with the result of Saffman & Schatzman (1982) (see (3.19) of their paper and note that $1{\cdot}705^{-\frac{1}{2}} \simeq 0{\cdot}77$ and $0{\cdot}5938^{-\frac{1}{2}} \simeq 1{\cdot}30$). This is the reason why we believe that the stable condition (3.30) may be reliable at least for $P \lesssim P_m$.

In the present approximation the shape of the vortex core is expressed by (2.31). In the case of an asymmetric configuration we are now considering, the velocity (u, v)

near the centroid of a vortex tube in the upper row induced by all the other vortices is written as

$$u(x,y) = \frac{\Gamma}{2l}\tanh\pi k - \frac{\Gamma\pi}{6l^2}(1-3\operatorname{sech}^2\pi k)\,y + \frac{\Gamma\pi^2}{2l^3}\frac{\sinh\pi k}{\cosh^3\pi k}(x^2-y^2) + O(S^2, x^3, x^2y, xy^2, y^3), \tag{3.39a}$$

$$v(x,y) = -\frac{\Gamma\pi}{6l^2}(1-3\operatorname{sech}^2\pi k)\,x - \frac{\Gamma\pi^2}{l^3}\frac{\sinh\pi k}{\cosh^3\pi k}xy + O(S^2, x^3, x^2y, xy^2, y^3), \tag{3.39b}$$

where (x,y) is the space co-ordinate relative to the centroid. Therefore the constants in (2.31) are calculated to be

$$A = D = 0, \quad B = -\frac{\Gamma\pi}{6l^2}(1-3\operatorname{sech}^2\pi k), \quad C = \frac{\Gamma\pi^2}{l^3}\frac{\sinh\pi k}{\cosh^3\pi k}. \tag{3.40}$$

The mean shape of a vortex tube without the free-oscillation terms is then given by

$$\langle r_b(\theta,t)\rangle = r_0\left[1+\tfrac{1}{3}\pi P(1-3\operatorname{sech}^2\pi k)\cos 2\theta + (\pi P)^{\frac{3}{2}}\frac{\sinh\pi k}{\cosh^3\pi k}\sin 3\theta\right], \tag{3.41}$$

which is symmetric in θ about $\theta = \frac{1}{2}\pi$. The vortex in the lower row has the same form, but is upside-down. The shapes for $k = k_c$ and $P^2 = 0{\cdot}02$ are plotted in figure 1.

4. Discussion

As conjectured by Christiansen & Zabusky (1973), if finite cores of vortex tubes are taken into account, there appears a stable region around $h/l = k_c$. However, since we are dealing with inviscid Navier–Stokes equations, which are time-reversible, the street is at most neutrally stable, i.e. there is no region where the growth rate is negative. The growth rate of the perturbation is given by

$$\mathscr{I}\lambda = \frac{\Gamma}{2\pi l^2}\mathscr{I}\Lambda, \tag{4.1}$$

where $\mathscr{I}\Lambda$ is obtained from (3.29). For $\phi = \pi$ and $k = 0$ we have

$$\mathscr{I}\lambda \simeq \frac{\pi\Gamma}{4l^2}(1-\tfrac{11}{6}\pi^2P^2). \tag{4.2}$$

For $\phi = \pi$ and $k = \infty$ we have

$$\mathscr{I}\lambda \simeq \frac{\pi\Gamma}{4l^2}(1+\tfrac{1}{6}\pi^2P^2). \tag{4.3}$$

These growth rates agree qualitatively with the numerical results of Christiansen & Zabusky (1973) that the growth rate is reduced at smaller values of k and increased at larger values of k by finite-core effects.

It is known experimentally that for the vortex streets behind a circular cylinder the spacing ratio changes with downstream distance (see Wille 1960). According to a recent measurement of Okude & Matsui (1981 private communication), the spacing ratio increases monotonically from 0·1 to a maximum value 0·45 between distances of

5 and 50 diameters downstream of a cylinder and then it seems to decrease gradually. We do not know where this discrepancy of the spacing ratio between theoretical and experimental values comes from. Probably the assumptions of infinite rows of vortex tubes and the uniform distribution of vorticity in vortex cores have to be checked first (Weihs 1972).

This work is partially supported by the Grant-in-Aid for Scientific Research from the Ministry of Education, Science and Culture. The author would like to thank Professor P. G. Saffman for sending him a copy of the paper Saffman & Schatzman (1982) prior to publication.

REFERENCES

Ahlfors, L. V. 1966 *Complex Analysis*, chap. 4, §6.2. McGraw-Hill.

Christiansen, J. P. & Zabusky, N. J. 1973 Instability, coalescence and fission of finite-area vortex structures. *J. Fluid Mech.* **61**, 219–243.

Domm, U. 1955 The stability of vortex streets with consideration of the spread of vorticity of the individual vortices. *J. Aero. Sci.* **22**, 750–754.

Goldstein, S. 1965 *Modern Developments in Fluid Dynamics*, vol. II, chap. XIII. Dover.

Kida, S. 1981 Motion of an elliptic vortex in a uniform shear flow. *J. Phys. Soc. Japan* **50**, 3517–3520.

Kochin, N. E., Kiebel, I. A. & Roze, N. F. 1964 *Theoretical Hydrodynamics*, chap. 5. Wiley Interscience.

Lamb, H. 1932 *Hydrodynamics*, 6th edn, chap. VII. Cambridge University Press.

Moore, D. W. & Saffman, P. G. 1971 Structure of a line vortex in an imposed strain. In *Aircraft Wake Turbulence and Its Detection* (ed. J. H. Olsen, A. Goldburg & M. Rogers), pp. 339–354. Plenum.

Okude, M. 1978 Experiments on the vortices in the wake behind a circular cylinder. Part 2. Rearrangement of the Kármán vortex street (in Japanese). *J. Japan Soc. Aero. Astro.* **26**, 377–384.

Saffman, P. G. & Schatzman, J. C. 1982 Stability of a vortex street of finite vortices. *J. Fluid Mech.* **117**, 171–185.

Taneda, S. 1959 Downstream development of the wakes behind cylinders. *J. Phys. Soc. Japan* **14**, 843–848.

Weihs, D. 1972 Semi-infinite vortex trails, and their relation to oscillating airfoils. *J. Fluid Mech.* **54**, 679–690.

Wille, R. 1960 Kármán vortex streets. *Adv. Appl. Mech.* **6**, 273–287.